The International Journal of Cardiovascular Imaging (2019) 35:57–65
https://doi.org/10.1007/s10554-018-1429-7

ORIGINAL PAPER

Left atrial mechanics in children: insights from new applications of strain imaging

Kyle D. Hope[1] · Yan Wang[1] · Maalika M. Banerjee[1,2] · Andrea E. Montero[1] · Natesa G. Pandian[2] · Anirban Banerjee[1]

Received: 7 May 2018 / Accepted: 30 July 2018 / Published online: 16 August 2018

Abstract

Our principal aim was to describe functional changes in dilated left atrium (LA) of children by using new applications of LA strain. We studied 66 patients (age range 0.2–22 years) consisting of 33 with LA enlargement. We utilized speckle-tracking imaging for assessment LA longitudinal strain (S) and longitudinal displacement (D). S–D loops were generated by plotting S and D data along Y and X axes, respectively. We also measured noninvasive LA stiffness index, $= \frac{E/e'}{LA\ peak\ strain}$ ($\%^{-1}$). Peak S in controls was 51.16 ± 19.45% versus 23.16 ± 13.66% in dilated LA ($p < 0.0001$). S–D loops in dilated LA group were significantly smaller compared to controls (2.62 ± 2.88 units vs. 5.24 ± 4.00 units, $p < 0.01$). Noninvasive LA stiffness index was higher in dilated LA group ($0.77 \pm 0.63\%^{-1}$ vs. $0.17 \pm 0.07\%^{-1}$, $p < 0.0001$). A cut-off LA stiffness value of $0.25\%^{-1}$ was found to maximize sensitivity and specificity (84.0% and 84.85%, respectively). Children with enlarged LA demonstrate decreased peak S, abnormal S–D loops and increased LA stiffness, providing a newer insight into LA function. Evaluation of LA mechanics may be applied in future as a surrogate for left ventricular filling parameters.

Keywords Left atrium · Left atrial mechanics · Left atrial stiffness · Left atrial strain · Strain–displacement loop

Abbreviations

STE	Speckle tracking echocardiography
LA	Left atrium
LV	Left ventricle
DICOM	Digital imaging and communications in medicine

Introduction

In adults, there is strong evidence that left atrial (LA) enlargement measured by echocardiography is a robust predictor of various cardiovascular outcomes [1, 2]. Numerous studies in adults have also evaluated left atrial physiology and function and correlated them with clinical conditions like heart failure and cardiomyopathies. However, in the pediatric population the LA represents the "forgotten" chamber of the heart and noninvasive studies on LA physiology and function in children are quite limited.

Studies of LA physiology have revealed a three-phase cycle, characterized by reservoir, conduit, and booster pump functions [3]. Noninvasive evaluation of LA physiology has been difficult in the past due to technical constraints and has been studied infrequently in children. However, with the advent of speckle-tracking echocardiography (STE), it is now possible to analyze some of these physiologic phases by quantifying LA deformation over the course of the entire cardiac cycle from a single beat. STE can generate both strain and displacement data from the same heart beat and may be useful in simultaneous assessment of regional and global myocardial deformation of a cardiac chamber. The longitudinal displacement of the LA wall indicates movement of the atrial wall away from or towards the centroid of the LA and may be considered as a surrogate for volume change. These parameters have been studied in various diseases in adults. Notably, in aortic stenosis longitudinal strain was noted to increase, while longitudinal displacement was noted to decrease from base to apex of the LV [4]. Based on these findings, we were enticed by the feasibility

✉ Anirban Banerjee
banerjeea@email.chop.edu

[1] Division of Cardiology, The Children's Hospital of Philadelphia, The Perelman School of Medicine at the University of Pennsylvania, 34th and Civic Center Boulevard, Philadelphia, PA 19104, USA

[2] Division of Cardiology, Tufts Medical Center, Tufts University School of Medicine, Boston, MA 02111, USA

of describing a strain–displacement (S–D) relationship in children with dilated LA in various diseased states.

In adults, the E/e′ ratio has been evaluated as a noninvasive marker for increased LV stiffness [5] and recent guidelines published by the American Society of Echocardiography (ASE) for evaluation of diastolic dysfunction in adults, define an E/e′ greater than 14 as being one of the key variables among others [6]. In contrast, in the pediatric population, the ASE diagnostic algorithms are not as reliable [7]. It is possible that in order to improve diagnostic accuracy of E/e′ ratio in children, further refinement of this ratio is needed. Recent studies have proposed LA stiffness as a potential surrogate for measuring LV diastolic function in adults [8]. The stiffness of left atrial myocardium is derived from the slope of the pressure-strain relationship [9]. Using this concept, Kurt et al. proposed that LA stiffness can be measured invasively as the ratio of the pulmonary capillary wedge pressure (PCWP) and peak LA strain. Kurt et al. also proposed a noninvasive method of measuring LA stiffness, where E/e′ was used in lieu of PCWP [8],

$$Noninvasive\ LA\ stiffness = \frac{E/e'}{Peak\ average\ LA\ strain}\ \left(\%^{-1}\right).$$

However, these parameters of LA stiffness are yet to be studied in children. We speculate that by correcting E/e′ with LA strain, noninvasive LA stiffness may improve the accuracy of E/e′ when applied for assessment of LV filling pressures in children and overcome the shortcoming of simply using E/e′.

The objective of our study is to characterize LA function throughout a single cardiac cycle in both normal and diseased states, using strain imaging and the strain–displacement relationship. We also wish to assess LA stiffness in the setting of normal and diseased LA. We hypothesize, that evaluation of LA strain in combination with LA displacement measured simultaneously during the same cardiac cycle, may provide useful insight into the function of both the normal and failing LA. We also propose that increased LA stiffness measured by a noninvasive technique may reflect increased LV filling pressures.

Methods

Patient population

For this retrospective study, normal subjects were recruited from children undergoing echocardiography for routine indications such as non-cardiac chest pain, benign syncope and benign heart murmurs. These patients had structurally and functionally normal hearts and were included in the control group. Due to the low incidence in the pediatric population, LA dilatation resulting from any etiology was accepted ("all comers" with LA dilatation), (Table 2). For defining LA dilatation, we followed the classification proposed by the Joint Writing Group of the American Society of Echocardiography (ASE) and European Association of Cardiovascular Imaging. Indexed LA volume was measured by area-length method from biplane two-dimensional echocardiography (2DE), (mild dilatation = 35–41 ml/m^2, moderate = 42–48 ml/m^2, severe = ≥ 48 ml/m^2) [10]. Demographic data were obtained from review of charts. This study was approved by the Institutional Review Board of the Children's Hospital of Philadelphia.

Echocardiographic studies

All echocardiographic studies were performed on Philips iE33 ultrasound machines (Philips Medical Systems, Andover, MA) and only those 2DE images acquired at frame rates > 60 Hz, were accepted for further analyses. Mitral inflow Doppler and mitral annular tissue Doppler velocities were derived from the septal and lateral sides of the mitral valve annulus and were averaged (e′). All patients were in sinus rhythm and patients under 6 months of age were excluded due to fusion of tissue-velocity e′ and a′ waves. We also excluded patients with mitral stenoses from analysis of LA stiffness, due to the presence of disproportionately high E waves in the latter group. None of the patients had undergone any cardiac surgery. To be consistent with previous studies, left ventricular end-diastole at the onset of QRS complex was defined as the starting point of the atrial cardiac cycle.

Strain imaging

Speckle tracking echocardiography (STE)

Digital imaging and communications in medicine (DICOM) clips of the 2DE apical four-chamber view were uploaded to a vendor-independent STE software (2D Cardiac Performance Analysis, TomTec Imaging Systems, version 1.1.3, Munich, Germany) for tracing the LA endocardial border. The TomTec LV software was utilized for measuring LA strain (due to lack of a dedicated LA software in the version of 2D Cardiac Performance Analysis used in this study). The LA tracing for strain was terminated 0.5 cm above the atrioventricular junction, to avoid influence of mitral annular motion. The entire LA wall and atrial septum was divided into six segments by the software. The software also generated longitudinal strain and longitudinal displacement data and corresponding waveforms from each segment from the same heart beat (Fig. 1). The averages of peak global strain and displacement values were used. By convention,

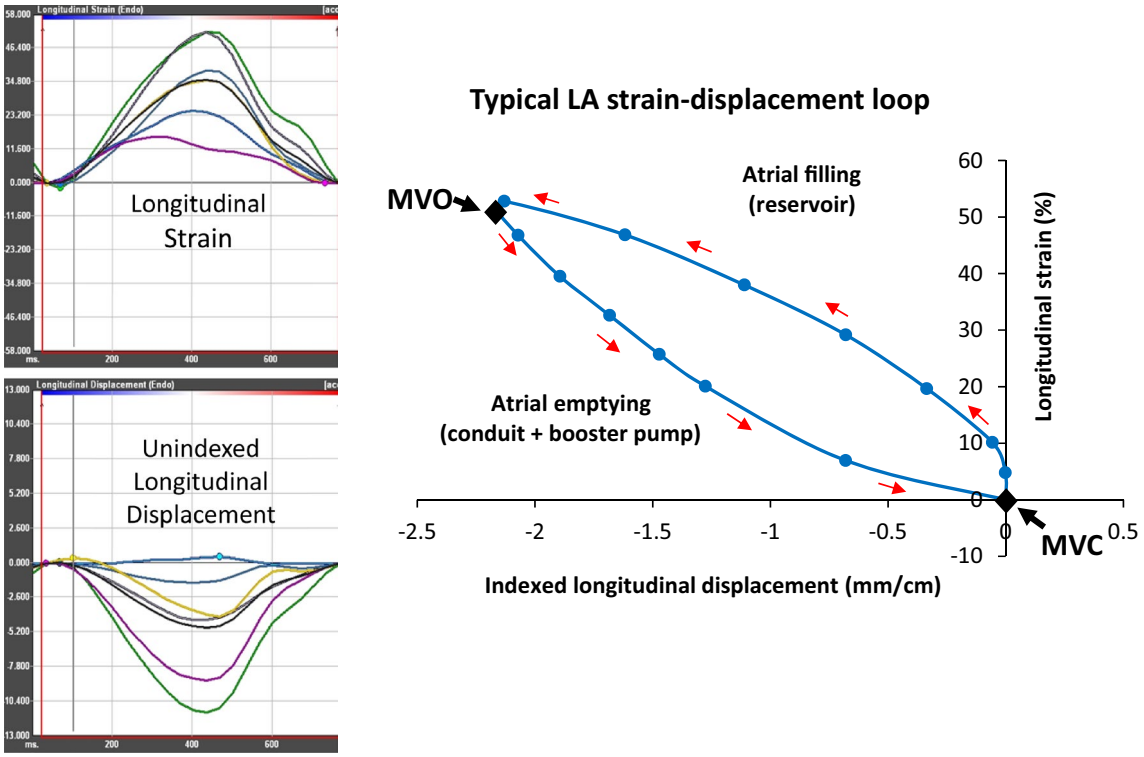

Fig. 1 Left atrial S–D loop was generated by plotting the LA longitudinal strain along the Y-axis and indexed longitudinal displacement along the X-axis. This results in a characteristic counter-clockwise, elliptical loop, starting with the mitral valve closure (MVC). The S–D loop was constituted by reservoir, conduit and contractile phases of LA function. The reservoir phase continues from MVC to mitral valve opening (MVO), after which starts the conduit phase, followed by a brief contractile phase. The contractile phase in children is not as pronounced as in adults and is not well detected in the wave forms, as it does not produce a distinct incisura

displacement away from the centroid of the cardiac chamber is indicated by negative values.

Construction of strain–displacement loops

The S–D loops were generated by plotting LA longitudinal strain along the y-axis versus longitudinal displacement along the x-axis. The purpose of constructing the S–D loop was to gain insight into all three phases of LA function from a single loop. To account for differences in the size of the LA between children of different ages, the longitudinal displacement was indexed by body surface area. In a second method, longitudinal displacement was indexed by dividing it with the largest LA dimension, as described previously by our group [11, 12]. The area enclosed by the S–D loop was calculated by dividing it into mini trapezoids, with the area of the loop equaling the sum of the areas of these trapezoids. This is known as the "trapezoidal area of polygon" formula and described as the sum of $[x(i+1)-x(i)][y(i)+y(i+1)]/2$ for i points of a polygon, where $x(1), y(1)=x(i+1), y(i+1)$ [13]. The unit for this measurement is %.mm/cm and is simply referred to as unit in this paper.

Noninvasive measure of LA stiffness

LA stiffness index was calculated from the following formula, to derive a dimensionless parameter: The E/e′ ratio was used in lieu of LA pressure to calculate LA stiffness noninvasively, as suggested by Kurt et al. [8].

$$LA\ stiffness\ index = \frac{E/e'}{LA\ peak\ strain}\ \left(\%^{-1}\right)$$

Cardiac catheterization data

We recorded PCWP measurements from the subset of patients that underwent diagnostic catheterization within 3 months of their echocardiograms. From these data correlations between noninvasive LA stiffness and PCWP were performed.

Statistical analysis

Continuous variables were reported as mean ± standard deviation (SD). Since the data were normally distributed,

comparisons between two variables were performed using Student's *t* test. Statistical analysis was performed using commercially available Stata software (StataCorp. 2011. *Stata Statistical Software: Release 12*. College Station, TX: StataCorp LP). Inter-observer and intra-observer analysis was assessed by intra-class correlation coefficients (ICC).

For generating cut-off values of LA stiffness, a receiver operator characteristic (ROC) curve was derived by plotting the sensitivity against 1-specificity. The area under curve (AUC) was calculated to assess the ability of LA stiffness to differentiate control patients from those with diseased states. A cut-off value was selected to maximize both sensitivity and specificity.

Results

Population demographics

A total of 66 patients were included in this study and clinical data are depicted in Table 1. LV ejection fraction was relatively preserved in the dilated LA group. LA enlargement was due to a number of etiologies, as described in Table 2. Of the patients with LA dilatation, 18% were classified as mild, 48% as moderate, and 33% as severe.

LA function

LA peak longitudinal strain differed significantly between the normal and dilated LA groups, with normal children demonstrating a mean peak longitudinal strain of 51.16 ± 19.45% compared to 23.16 ± 13.66% in the dilated group, $p < 0.0001$ (Table 3). The S–D loop had a characteristic elliptical shape and counterclockwise rotation, and was reflective of the reservoir, conduit, and contractile phases of LA function (Fig. 1). The reservoir phase began with MVC and continued until mitral valve opened (MVO). The conduit phase began at MVO and was followed by a brief contractile (booster pump) phase. The contractile phase in children is not as pronounced as in adults and was not well detected in both the wave forms due to lack of a distinct incisura.

Table 1 Demographic, clinical, and echocardiographic characteristics

	Control n = 33	Dilated LA n = 33	p Value
Age (y)	11.46 ± 13.00	10.55 ± 6.98	
Male	16 (48%)	15 (45%)	
Mitral E (m/s)	1.04 ± 0.22	1.37 ± 0.62	0.006
Average e′ (m/s)	0.14 ± 0.02	0.10 ± 0.03	< 0.001
E/e′ ratio	7.55 ± 2.22	11.20 ± 4.62	0.001
E/A ratio	2.04 ± 0.68	2.06 ± 0.78	0.95
LVEF (%)	63.63 ± 7.25	55.55 ± 15.46	0.01
LVSF (%)	38.12 ± 4.90	32.63 ± 10.34	0.01
LV longitudinal strain (%)	− 20.40 ± 3.57	− 17.39 ± 5.81	0.01

BSA body surface area, *LVIDd* LV internal dimension in diastole, *LVED* LV end diastolic, *Average e′* average of lateral and septal tissue Doppler imaging e′, *LVEF* LV ejection fraction, *LVSF* LV shortening fraction

Data are expressed as mean ± standard deviation

Table 2 Etiology of left atrial dilatation

Etiology of LA dilatation	Number of patients (n = 33)
Mitral valve regurgitation	12
Mitral valve stenosis	2
Dilated cardiomyopathy	5
Left-to-right shunt	5
Restrictive cardiomyopathy	4
Hypertrophic cardiomyopathy	5

The S–D loop also showed a second distinctive pattern, labeled as the "figure-of-eight" pattern (Fig. 2). This pattern was noted in a subset of patients in both control group (42%) and dilated LA group (36%). In the figure-of eight group, the longitudinal displacement ended 67 ± 23 ms earlier than in the elliptical group. The implications of these two types of loops will be discussed later.

Notable differences emerged when S–D loops from normal children were compared to those with dilated LA due to diseased states. The S–D loops in diseased patients with a dilated LA were significantly smaller in size compared with normals (Fig. 2). The average area enclosed by the S–D loop differed significantly between the normal and dilated LA groups (5.24 ± 4.00 vs. 2.62 ± 2.88 units, $p < 0.01$) as shown in Fig. 3.

Noninvasive LA stiffness index was also significantly different between the normal and diseased groups (Table 3). To evaluate its role as a potential tool for differentiating these two groups, ROC curves were generated with resultant AUC of 0.89 (95% confidence interval 0.80–0.98), (Fig. 4). A LA stiffness cut-off value of $0.25\%^{-1}$ was found to maximize sensitivity and specificity for differentiating patients with dilated LA from normal controls, with values of 84.0% and 84.8%, respectively.

Cardiac catheterization data were available in 15 patients in the dilated LA group and showed a statistically significant curvilinear relationship between PCWP and noninvasive LA stiffness. An exponential relation provided the best fit for the data ($r = 0.78$, $p < 0.01$, Fig. 5).

Table 3 Left atrial data

	Control	Dilated LA	p Value
LA peak longitudinal strain (%)	51.16 ± 19.45	23.16 ± 13.66	< 0.0001
LA S–D loop area (units)	5.24 ± 4.00	2.62 ± 2.88	< 0.01
Noninvasive LA stiffness index ($\%^{-1}$)	0.17 ± 0.07	0.77 ± 0.63	< 0.0001

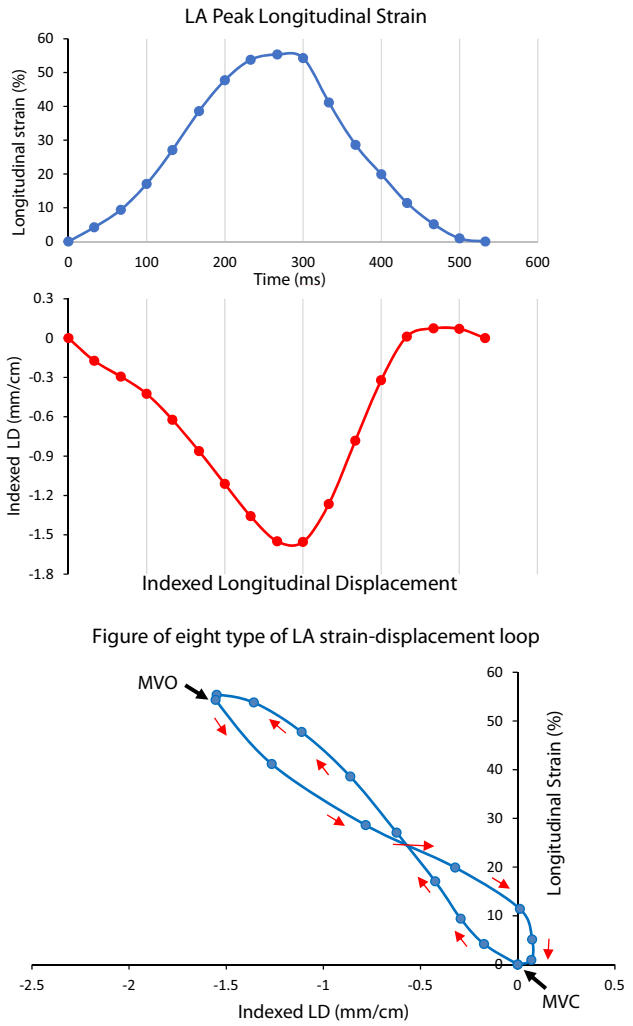

Fig. 2 A figure-of-eight type of SD loop is depicted here. It was generated by plotting the LA longitudinal strain along the Y-axis and indexed longitudinal displacement along the X-axis The longitudinal strain and displacement curves are shown in the panels above the loop. *MVC* mitral valve closure, *MVO* mitral valve opening

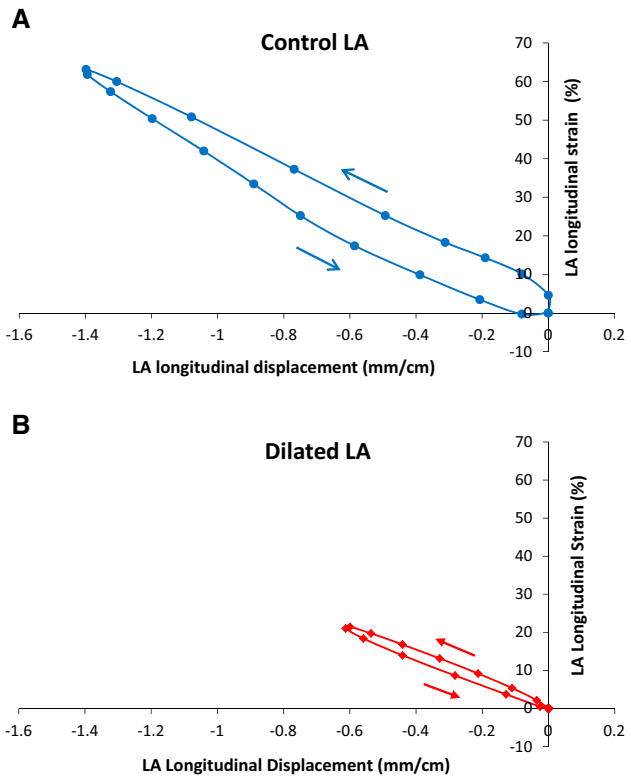

Fig. 3 Left atrial strain–displacement loops, in a normal (**a**) and in a diseased LA (**b**). The longitudinal displacement is indexed to the LA length measured at LV end-systole, when the dimension of the LA is largest

Intra-observer and inter-observer variability

ICC coefficient of 0.82 was calculated for serial measurements of LA strain. Similarly, inter-observer variability was assessed by two investigators. For inter-observer variability, ICC coefficient of 0.85 was calculated, indicating good agreement between the two observers.

Discussion

This pilot study provides a new approach for evaluating LA mechanics in normal and diseased states in children. To our knowledge, this is the first study in children that describes the concept of S–D loops and LA stiffness index, in both normal and diseased states of the LA. The S–D loop reflects all three phases of LA cycle measured from a single beat. Those patients with enlarged LA demonstrate decreased longitudinal strain, small S–D loops and an increased LA stiffness index.

Left atrial function

Measurement of LA strain represents an exciting new tool in the assessment of LA physiology that was not available

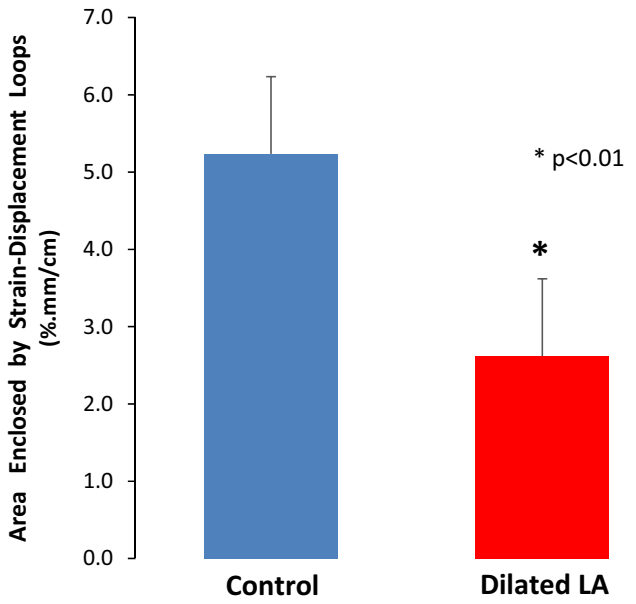

Fig. 4 Area enclosed by LA strain–displacement loops in controls and in dilated LA in diseased states. The error bars represent standard error of mean

in the past. Our data demonstrate a significant difference in the magnitudes of LA strain between control and diseased states. This preliminary study may provide a basis for newer studies assessing the role of the LA in cardiac dysfunction in the pediatric population.

LA strain–displacement loops

A new physiologic approach of this study was the construction of characteristic LA S–D loops with turning points corresponding to mitral valve closing and opening (Figs. 1, 2). Strain represents local deformation of a small myocardial segment, whereas, displacement evaluates the movement of the whole-chamber. The S–D loops may serve as a helpful index comparing atrial segmental deformation against the overall movement of the atrial wall and may provide a useful "composite view" of atrial filling (reservoir phase) and emptying (conduit + contractile phases). The concept of simultaneous measurement of longitudinal strain and displacement has been applied in adults with constrictive pericarditis [14], right ventricular pressure overload [15, 16] and in the evaluation of carotid artery stiffness [17]. Longitudinal strain and displacement have been used to describe the elasticity of the dilated aorta. Elasticity of the aorta incorporates both the property of dilating and the property of recoiling to its initial shape [18]. Similarly, the atrial strain–displacement relationship may provide indirect evidence of the elasticity of the atrial tissue. We also speculate that during the conduit phase (when mitral valve remains open), the LA S–D loop may also reflect LV diastolic stiffness. We have applied the concept of S–D relationship in the right atrium of children with primary pulmonary hypertension, where it was able to identify patients who are at risk for future adverse outcomes associated with right ventricular failure [12].

Based on the present study we speculate that the reduced area of the S–D loop may provide a visual display of the decreased elasticity of the stretched atrial tissue in a dilated

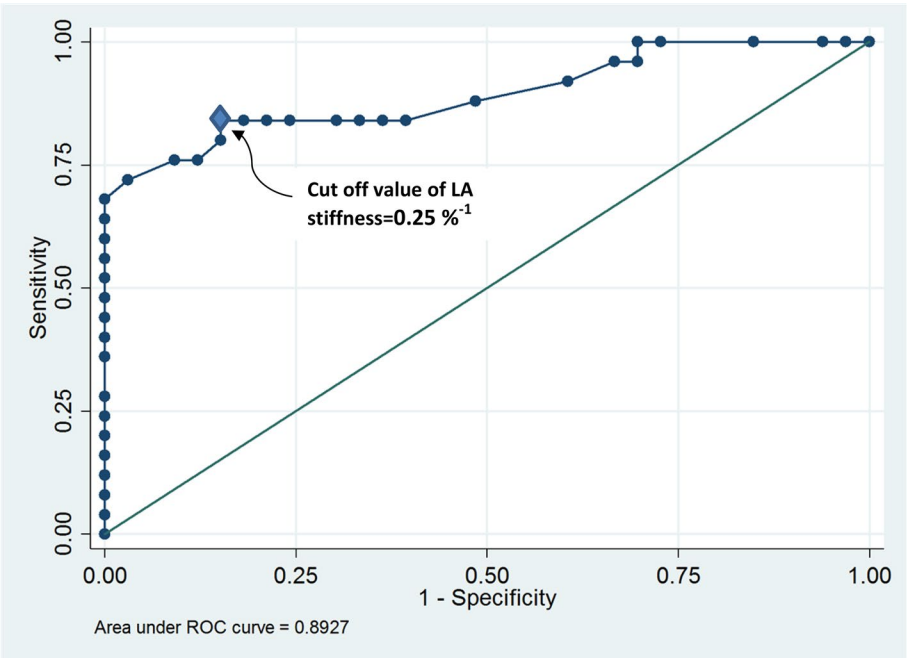

Fig. 5 Receiver operating characteristic curve showing the role of LA stiffness index in differentiating the LA from diseased patients versus normal controls. Area under curve (AUC) is 0.89 (95% confidence interval 0.8–0.98). LA stiffness cut-off value of $0.25\%^{-1}$ was found to maximize sensitivity and specificity with values of 84.0 and 84.85%, respectively

LA (Fig. 3). However, this is a pilot study that aimed to show the feasibility of constructing S–D loops in normal and dilated LA. To transfer this physiologic data to clinical data, would clearly require further studies of S–D loops in different disease states.

The S–D loops in ours study had two different shapes: (1) elliptical or (2) figure-of-eight. The exact mechanisms that produce these different patterns are not clear from our study. We speculate that the elliptical pattern was created by synchronized decrease in both strain and displacement, after the opening of the mitral valve. In contrast, the figure-of-eight pattern may be the consequence of slower decrease in longitudinal strain after MVO. In this group, we also noted that the longitudinal displacement ended earlier and the displacement curve became quiescent for a brief period prior to MVO. There may be other factors that may play a role in generating the figure-of-eight loop. The end result is a descending limb of the loop that is less steep and crosses the ascending limb to produce a figure-of-eight pattern. Due to a limited number of patients in each sub-group, more detailed sub-group analysis of these loops, regarding age, size of the LA etc. was not feasible. However, since this pattern was noted in a sizeable number of patients in the control group, we can merely speculate that that the figure-of-eight pattern may represent a normal variant. LA pressure volume-loops generated by invasive instrumentation in the normal canine model, also have a figure-of-eight appearance [19]. In normal children, during the construction of torsion–displacement loops we have also noted such figure-of eight patterns during untwisting of the LV [20].

Role of LA stiffness

Studies in adults have depicted an inverse correlation between LA strain and mean wedge pressure obtained by catheterization [21]. In our limited subgroup analysis, we found a good correlation between the new concept of non-invasive LA stiffness and PCWP. Moreover, the curvilinear relationship made prudent physiologic sense, suggesting that LA stiffness increases more steeply at very high LV filling pressures.

Over more than 15 years, E/e′ ratio has been used successfully in adults as one of the important noninvasive indices among others, for predicting LV filling pressures. The most recent guidelines published by the ASE, suggest a cut-off value of E/e′ ratio of > 14 be used as one of the criteria to accurately predict elevated LA pressures (Grade III diastolic dysfunction) [6].

However, the E/e′ ratio is not as reliable in children with LV diastolic dysfunction as it is in adults. In fact, in children with various types of cardiomyopathies criteria for diastolic dysfunction were discrepant in a majority of patients and half of the patients exhibited E/e′ values that were within the normal range for age [7]. In the pediatric age group, the E/e′ ratio showed significant overlap between normal patients and those with established diagnoses of dilated, hypertrophic and restrictive cardiomyopathies. While recent data have established normal values for tissue Doppler parameters in healthy children [22, 23], no consensus has yet been reached on which values indicate elevated LV filling pressures.

The adult progression of diastolic dysfunction proceeds through a continuum, characterized by delayed relaxation, followed by a pseudo-normal filling pattern and, thereafter, transitioning to a restrictive filling pattern. Progression of these pathophysiologic changes may be captured at each stage by established echocardiographic criteria in adults [24]. However, the diagnosis and progression of diastolic dysfunction in children using these adult ASE guidelines remain poorly defined, for example, E/A wave reversal is quite infrequent in children with established diastolic dysfunction.

To aid in quantifying elevated LV filling pressures in the pediatric population, we propose the use of LA stiffness index as an additive parameter which may improve the accuracy of E/e′ ratio when applied in children. In adults, E/e′ has been used in lieu of LA pressure to calculate LA stiffness [8] and we have borrowed this concept and the term from our adult counterparts. At the same time, we are aware of the shortcomings of applying E/e′ in children. Therefore, our goals were more modest compared to studies performed in adults. In this study, we wished to improve the usefulness of E/e′ by combining it with peak LA strain and create a new index (LA stiffness) that may have incremental value over E/e′. In our study, the LA stiffness index demonstrated a distinct cutoff value ($0.25\%^{-1}$), in the diseased group with good sensitivity and specificity. It is true that measurement of LA stiffness is not necessary for diagnosing LA enlargement. However, increase in LA size and LA stiffness may go hand in hand in response to increased LV filling pressures. Increase LA stiffness may detect increase in LV filling pressures (Fig. 6).

In adults suffering from heart failure with preserved ejection fraction (HFpEF), LA dilatation is often considered a hallmark of LV diastolic dysfunction [25]. We wish to point out that we have used the model of a dilated LA to serve as surrogate for impaired atrio-ventricular coupling, in conditions where LV systolic function is preserved. Our description of LA stiffness was intended to describe a new physiologic parameter that could be applied in the clinical arena in the future. It is our hope that future studies will be pursued in children to validate this new concept in a wider spectrum of cardiac conditions, like in different types of cardiomyopathies that result in significantly elevated LV filling pressures. Invasive validation of LA stiffness using catheterization data, was not a primary goal of this study as this is a retrospective study and we were aware that

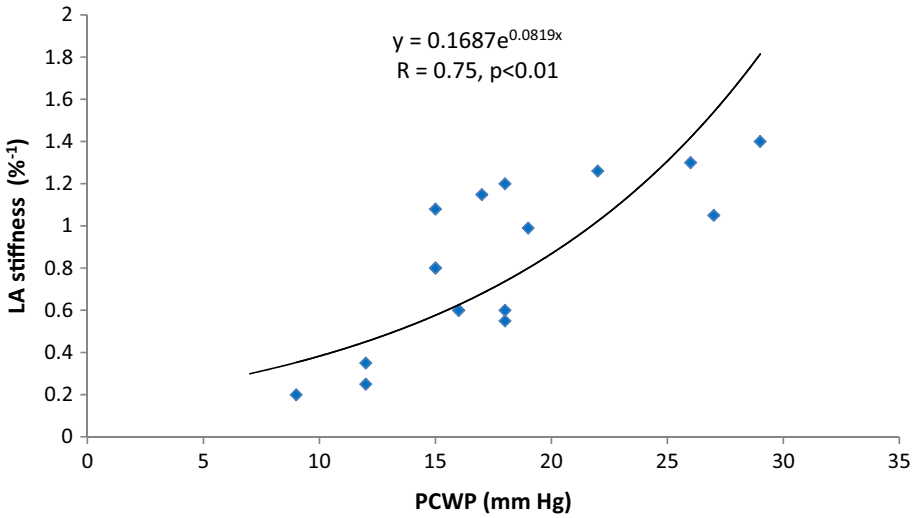

Fig. 6 Correlation between PCWP and LA stiffness. An exponential relationship provided the best fit for the data and showed a statistically significant curvilinear relationship between the two variables ($r = 0.78$, $p < 0.01$). The LA stiffness increased dramatically at higher PCWP

diagnostic catheterization data would not be available in all our patients. Therefore, we have simply reported the PCWP data that were available in a subset of patients.

Study limitations

We used "all comers" for patient recruitment since the incidence of LA dilatation is much less in children compared to adults, even at a large tertiary, pediatric cardiac center. This is an inherent limitation of performing research in children. Due to this shortcoming, the patients with enlarged LA form a heterogeneous group of patients. Since this is a preliminary study, it was important to include as many patients with LA enlargement as possible. Longitudinal studies may shed additional light on the changes in S–D loops measured in the same patient over time. The small sample size of each subset of patients, precluded further sub-group analysis e.g. etiological differences, pressure- vs. volume-overload or between age groups. The current trend of performing limited number of diagnostic catheterizations in children, is reflected in our LA stiffness-PCWP analysis, where only small number of patients in whom LA stiffness was evaluated, also had catheterization data.

In adult studies, LA reservoir, conduit and pump functions have been reported using various parts of the LA strain curve. In adults, the LA *reservoir* function has been calculated typically from peak LA strain, which was also measured in our study. However, we chose not to calculate *conduit* or *booster pump* functions due to lack of a distinct incisura on the strain curve of children that depicted the onset of the pump function. Finally, measurements of LA stiffness and construction of S–D loops represent new advancements in assessing atrial mechanics. Future studies are needed to further validate our preliminary observations.

Clinical implications

The mathematical calculations for measuring these indices can be incorporated into calculation packages of commercial echocardiography machines. Automation of S–D loops and stiffness indices into commercial ultrasound machines may encourage more use of these indices in busy clinical settings and not limit them to the research arena only. In adults along with E/e′ ratio, dilatation of the LA maximal volume is also a key variable utilized in identifying diastolic dysfunction [6, 25]. However, the measurement of LA volume is not as prevalent in pediatric cardiology. Nevertheless, dilatation of the LA should be considered an important characteristic of diastolic dysfunction. Using the dilated LA as an indirect consequence of diastolic dysfunction, we have proposed the use of S–D loops and LA stiffness to serve as additional variables for detecting diastolic dysfunction in children.

Conclusions

Simultaneous measurement of LA longitudinal strain and displacement from the same cardiac cycle, may provide a new insight into LA mechanics. Increased LA stiffness index $> 0.25\%^{-1}$ may suggest increased LV filling pressures. Evaluation of LA mechanics may serve as an indirect method of evaluating LV filling parameters in children.

Acknowledgements We wish to thank Ms. Xuemei Zhang of the Children's Hospital of Philadelphia, for providing statistical help for our study.

Funding This research did not receive any grant from funding agencies in the public, commercial, or not-for-profit sectors.

Compliance with ethical standards

Conflict of interest None of the authors have any conflict of interest that could have influence the manuscript.

Ethical standards This study was approved by the Institutional Review Board of The Children's Hospital of Philadelphia.

Informed consent Informed consent was not obtained as this was a retrospective study.

References

1. Tsang TSM, Barnes ME, Gersh BJ et al (2003) Prediction of risk for first age-related cardiovascular events in an elderly population: the incremental value of echocardiography. J Am Coll Cardiol 42(7):1199–1205
2. Leung DY, Boyd A, Ng AA, Chi C, Thomas L (2008) Echocardiographic evaluation of left atrial size and function: current understanding, pathophysiologic correlates, and prognostic implications. Am Heart J 156(6):1056–1064
3. Abhayaratna WP, Seward JB, Appleton CP et al (2006) Left atrial size: physiologic determinants and clinical applications. J Am Coll Cardiol 47(12):2357–2363
4. Cramariuc D, Gerdts E, Davidsen ES, Segadal L, Matre K (2010) Myocardial deformation in aortic valve stenosis: relation to left ventricular geometry. Heart 96(2):106–112
5. Nagueh SF, Middleton KJ, Kopelen HA, Zoghbi WA, Quinones MA (1997) Doppler tissue imaging: a noninvasive technique for evaluation of left ventricular relaxation and estimation of filling pressures. J Am Coll Cardiol 30:1527–1533
6. Nagueh SF, Smiseth OA, Appleton CP et al (2016) Recommendations for the evaluation of left ventricular diastolic function by echocardiography: an update from the American Society of Echocardiography and the European Association of Cardiovascular Imaging. J Am Soc Echocardiogr 29(4):277–314
7. Dragulescu A, Mertens L, Friedberg MK (2013) Interpretation of left ventricular diastolic dysfunction in children with cardiomyopathy by echocardiography: problems and limitations. Circ Cardiovasc Imaging 6:254–261
8. Kurt M, Wang J, Torre-Amione G, Nagueh SF (2008) Left atrial function in diastolic heart failure. Circ Cardiovasc Imaging 2(1):10–15
9. Hoit BD (2008) Left atrial function: basic physiology. In: Klein AL, Garcia MJ (eds) Diastology: clinical approach to diastolic heart failure. Saunders Elsevier, Philadelphia, pp 33–41
10. Lang RM, Badano LP, Mor-Avi V et al (2015) Recommendations for cardiac chamber quantification by echocardiography in adults: an update from the American Society of Echocardiography and the European Association of Cardiovascular Imaging. J Am Soc Echocardiogr 28(1):1–39
11. Nawaytou HM, Yubbu P, Montero AE et al (2016) Left ventricular rotational mechanics in children after heart transplantation. Circ Cardiovasc Imaging 9(9):e004848
12. Hope KD, Calderón Anyosa RJC, Wang Y et al (2018) Right atrial mechanics provide useful insight in pediatric pulmonary hypertension. Pulm Circ 8(1):2045893218754852. https://doi.org/10.1177/2045893218754852
13. Area of a Trapezoid [Internet article] (2012). http://www.aaamath.com/geo78_x5.htm. Accessed 8 Aug 2016
14. Negishi K, Popović ZB, Negishi T et al (2015) Pericardiectomy is Associated with Improvement in Longitudinal Displacement of Left Ventricular free wall due to increased counterclockwise septal-to-lateral rotational displacement. J Am Soc Echocardiogr 28:1204–1213
15. Ichikawa K, Dohi K, Sugiura E et al (2013) Ventricular function and dyssynchrony quantified by speckle-tracking echocardiography in patients with acute and chronic right ventricular pressure overload. J Am Soc Echocardiogr 26:483–492
16. Urheim S, Cauduro S, Frantz R et al (2005) Relation of tissue displacement and strain to invasively determined right ventricular stroke volume. Am J Cardiol 96:1173–1178
17. Tat J, Au JS, Keir PJ, MacDonald MJ (2015) Reduced common carotid artery longitudinal wall motion and intramural shear strain in individuals with elevated cardiovascular disease risk using speckle tracking. Clin Physiol Funct Imaging 37(2):106–116. https://doi.org/10.1111/cpf.12270
18. Bieseviciene M, Vaskelyte JJ, Mizariene V et al (2017) Two-dimensional speckle-tracking echocardiography for evaluation of dilative ascending aorta biomechanics. BMC Cardiovasc Disord 17(1):27. https://doi.org/10.1186/s12872-016-0434-9
19. Hoit BD, Shao Y, Gabel M et al (1994) In vivo assessment of left atrial contractile performance in normal and pathological conditions using a time-varying elastance model. Circulation 89(4):1829–1838
20. Di Maria MV, Caracciolo G, Prashker S et al (2014) Left ventricular rotational mechanics before and after exercise in children. J Am Soc Echocardiogr 27(12):1336–1343
21. Wakami K, Ohte N, Asada K et al (2009) Correlation between left ventricular end-diastolic pressure and peak left atrial wall strain during left ventricular systole. J Am Soc Echocardiogr 22(7):847–851
22. Dallaire F, Slorach C, Hui W et al (2015) Reference values for pulse wave Doppler and tissue Doppler imaging in pediatric echocardiography. Circ Cardiovasc Imaging 8:e002167
23. Cantinotti M, Giordano R, Scalese M et al (2016) Nomograms for mitral inflow Doppler and tissue Doppler velocities in Caucasian children. J Cardiol 68(4):288–299
24. Nagueh SF, Appleton CP, Gillebert TC et al (2009) Recommendations for the evaluation of left ventricular diastolic function by echocardiography. J Am Soc Echocardiogr 22:107–133
25. Melenovsky V, Borlaug BA, Rosen B et al (2007) Cardiovascular features of heart failure with preserved ejection fraction versus nonfailing hypertensive left ventricular hypertrophy in the urban Baltimore community: the role of atrial remodeling/dysfunction. J Am Coll Cardiol 49(2):198–207